

A Simple Model for DoD Inkjet Frequency Response

Stephen D Hoath; University of Cambridge, Department of Engineering; Cambridge, United Kingdom

Abstract

A simple linear model of piezo DoD inkjet print-head jetting output (drop speed, volume, momentum) provides an analytic prediction for the frequency response for steady state and initial printing streams from nozzles. The model has been applied to both existing commercial and development inkjet print-head devices.

Introduction

As a result of the industrial marketing push towards ever higher inkjet printing (jetting) frequencies and smaller drop sizes, and the rapid progress being made in applications of MEMS-based manufacturing, some drop-on-demand (DoD) inkjet print head designs rely on piezo-actuated (driven) resonant chambers to generate liquid droplets. The resonant oscillations set up residual pressure waves as a result of simple actuation drive pulses, e.g. see Bogy and Talke (1984) [1], Dijksman (1984) [2], Dijksman and Pierik (2012) [3] and these have to be tamed by a combination of print-head design and/or by waveform modifications, e.g. Wijshoff (2010) [4], Khalate et al (2011) [5] and (2012) [6], and as described within [7]. We will focus here on the piezo DoD print-head output, which for most inkjet users is the drop speed and the drop volume that is achieved for a specific range of frequencies.

Residual response

Piezo-based DoD print-heads are generally actuated by means of piezoelectric materials to which voltage is applied (or removed). For resonant devices, the print-heads include main chambers with inlets and outlets for ink supply and jetting nozzles. In the simplest case, in which refill modes are ignored, the main chamber and jet nozzle can be represented as a single Helmholtz resonator having a frequency f_H and Q-factor Q . Print-heads have mechanically (and fluidic) coupled arrays of such chambers and both jetting and non-jetting nozzles, so finite cross-talk between neighboring channels can seriously disrupt the output of a specific channel (or pin#).

Using the well-known exponentially decaying form of residual waves associated with a damped single mode resonant chamber after completion of a (piezo-driven) drop-on-demand print-head actuation pulse, the effect of any number of similar pulses can be computed analytically, in the absence of any dynamic changes, by simple summation of terms, as found for linear superposition of waves in many other physical systems. This simple method completely ignores the details of the actuation pulse duration, but changes to the shape of the frequency response introduced by more realistic representations of the “waveform” are found to be rather small. Therefore the simple model results presented here provide a standard basis to benchmark DoD inkjet print-head designs.

Multi-pulse train modelling is deceptively simple in principle, because it assumes a linear response. There is plenty of evidence for such behavior in the academic literature [8, 9] reporting DoD drop speeds and drop volumes are linear in the piezo drive voltage. The multi-pulse trains can be single pulses repeated at a constant

frequency, or structured pulses having ‘grayscale’ sub-drops with fixed time spacing that are also repeated at a constant frequency. Compensation pulses and modified pulse amplitudes or structured timing within a ‘single’ pulse, and influence of multi-pulse trains on the other nozzle residuals (‘cross-talk’) can be easily modelled by appropriate adaptations of the multi-pulse train approach.

To understand experimental frequency sweep responses of inkjet print-heads first assume that the print-head output behavior (drop speed and volume) is linear in the applied drive voltage, as ink drops are known to behave like this at low print rates for DoD print heads from a wide range of manufacturers. The linear models predict print-head frequency dependence by making summations over suitable multi-pulse trains. The drop speed and volume are then proportional to drive voltage and each other at all frequencies.

Whatever the precise pulse-train formation, it appears that the multi-pulse train approach allows very simple, calculable and exact analytic prediction results for steady state and ‘first drop’ behavior over all frequencies. Thus the predictive power of the model derives from the linear assumption and exact results for the (normalized) drop speed and volumes jetted by chambers with independently specified f_H and Q .

From this baseline, experimental results probe and measure the assumptions of linearity, f_H and Q ; they have already been used to help identify some early prototype print-head build quality issues. Furthermore the linear multi-pulse train model explains many features of the observed drop speed and drop volume over the whole range of print frequencies up to and in some instances beyond f_H . One early success of the multi-pulse train model showed that the actual response to a drive voltage with a uni-modal pulse duration measured by the pulse width at half height (PW) did correspond closely to the optimum value (OPW) for the resonant chamber: $OPW = \frac{1}{2} / f_H$ even when $PW \neq OPW$. This experimental fact helped simplify the mathematics (presented below) but is not intrinsic to the linear assumption and the physics of the chamber response to being driven off-resonance: driving at (or close to) peak requires lower drive voltage than that needed for the same output off-resonance. Likewise the Q-factor influences the efficiency of the piezo-driven print-head, but given the value of Q (and f_H) does not influence the form of the frequency response.

Derivation

The resonant response of the DoD print-head to single 1 dpd (sub-drop per drop) pulse excitation is assumed to be proportional to a single, exponentially-damped, cosine term after a time t :

$$\cos(2\pi f_H t) \exp(-\pi f_H t / Q) \quad (1)$$

The cosine term in (1) shows that the response involves the chamber resonant frequency f_H . The $\pi f_H / Q$ in (1) is controlled by the damping factor $\zeta = 1 / (2Q)$, where $0 \leq \zeta < 1$ will permit residual oscillations. For damping ζ with a low $Q > \frac{1}{2}$, the oscillation

frequency is lowered to $f_H \sqrt{1-\zeta^2}$, but in piezo DoD inkjet print-heads the damping correction to this frequency can be neglected. The residual decays to $e^{-\pi} \approx 4.32\%$ after a time equivalent to the 'flat background' frequency $B = f_H/Q$. Since inkjet print-head drop speed specifications are typically $\pm 5\%$ or better, B is a reasonable estimate for the expected low frequency range for a flat response, although a lower flat frequency band may be anticipated ($B/2$) for precision applications. Q is approximately the number of oscillation cycles occurring before the residual response dies away to $e^{-\pi} \approx 4.32\%$. Figure 1 displays the decay with time for case $Q=9$; Figure 2 shows the steady state frequency response for this case and Figure 3 compares these for cases $Q=3, 6$ and 9 according to the multi-pulse train results predicted by equation (2) below.

Actuation responses are summed linearly over all the earlier decaying responses (see Appendix below for the underlying math); for multi-pulse trains of frequency f , response $R(f)$ is given in the steady state limit, with $a = 2\pi f_H \sqrt{1-1/(2Q)^2} f$ and $b = \pi f_H / (Qf)$, by

$$R(f) = (1 - \cos(a)\exp(-b)) / (1 + \exp(-2b) - 2\cos(a)\exp(-b)) \quad (2)$$

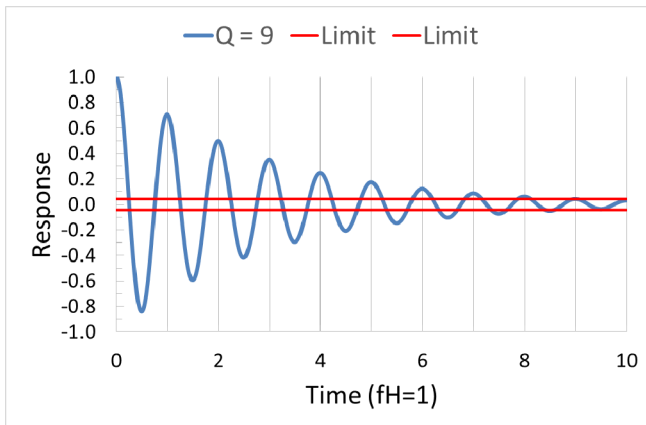


Figure 1. Decay of residual response for $Q=9$ during time after a single pulse. Dimensionless time units ($fH=1$) are used so that one cycle takes 1 time unit. Horizontal limit lines at $\pm \exp(-\pi)$ represent some typical speed specifications.

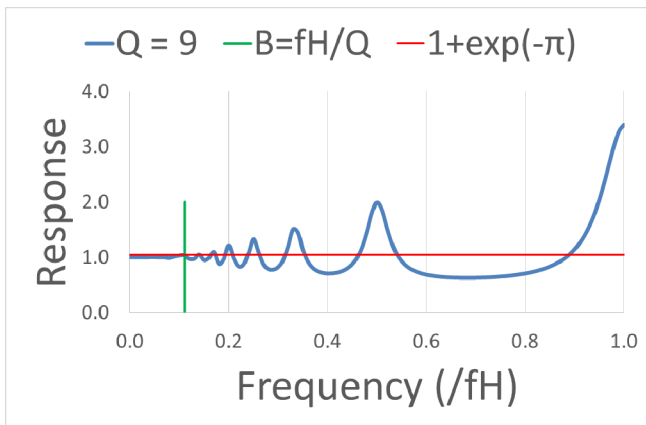


Figure 2. Predicted frequency response for DoD print-head system of Figure 1. Flat bandwidth $B = 1/9$ for frequency unit $fH=1$. Response can be interpreted as drop speed or volume ($= 1$ unit at low f). Typical drop speed ranges are shown.

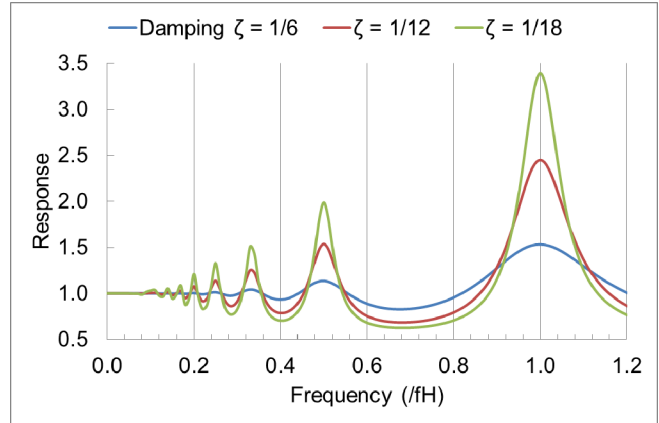


Figure 3. Jetting frequency response modelled for a resonant system of natural frequency $fH=1$ & Q -factors of 3, 6 or 9 ($\zeta = 1/6, 1/12$ or $1/18$, respectively). The efficiency for driving the resonant chamber at sub-harmonic peaks, rather than at lower frequencies, evidently increases with Q -factor, but drop response variations are also increased. (Note suppressions for clarity: the response axis 0.0 and small shifts for the low Q peak frequencies due to the factor $\sqrt{1-\zeta^2}$.)

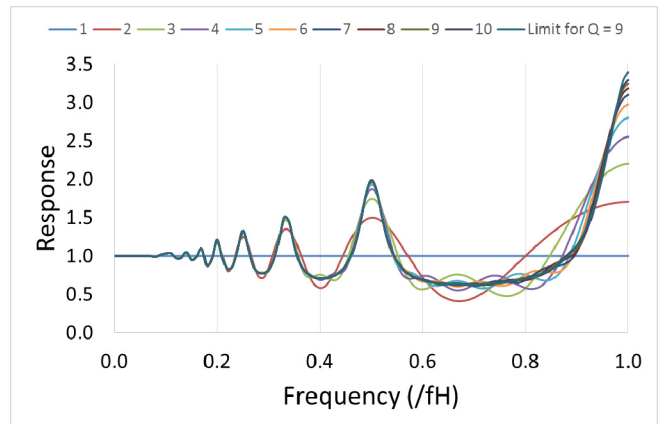


Figure 4. Predicted N^{th} drop frequency response for the print-head of Figure 1. The response for $N=1$ is flat, but as N increases the frequency spectrum will build systematically towards the steady state limit shown. For $Q=9$ as Figure 1. At frequencies below the $m=2$ sub-harmonic of f_H , the main changes predicted will arise due to the difference between the first and second drop responses.

Multi-pulse trains can also be used to predict the response $R(N, f)$ after N pulses at fixed frequency f :

$$R(N, f) = \{(1 - \cos(a)\exp(-b))(1 - \cos(Na)\exp(-Nb)) + (\sin(a)\sin(Na)\exp(-(N+1)b))\} / \{1 + \exp(-2b) - 2\cos(a)\exp(-b)\} \quad (3)$$

When Nb is sufficiently large that $\exp(-Nb) \ll 1$, equation (3) can be replaced, for all practical purposes, by the simpler equation (2).

Figures 2 and 3 are steady state predictions computed using equation (2), whereas Figure 4 for $Q=9$ is based on equation (3) and displays frequency responses for the scenario that $N = 1$ to 10 jetted drops can be measured at any given printing frequency. Figure 4 also shows the $N \rightarrow \infty$ steady state limit from equation (2).

The most obvious response variations arise where printing frequency f equals the m -th sub-harmonic frequency f_H/m of the basic frequency: peaks at $m \geq 2$; lows at $m > \frac{1}{2}(2n+1)$ for $n > 0$. Printing may prove advantageous at such sub-harmonic peaks [10].

An intrinsic “Nth-drop” effect emerges from equation (3), which is both Q-factor and frequency-dependent. Figure 4 shows the case for one particular $Q=9$, which confirms that the printing of at least $N=Q$ drops is required for the response to approach the steady state solution of equation (2). This intrinsic requirement is in addition to the observed “first-drop” effects often attributed to physical changes in the ink that may arise from solvent volatility, dynamic surface tension, clogging, temperature changes, viscosity, humidity, air ingress, etc., during non-printing periods. However, as the N-dependency effect is intrinsic and predictable it could, in principle, be properly taken into account within printing software.

Application to commercial DoD print-heads

Measurements of the drop speed for single pulses (not corresponding to specific waveforms developed for real DoD applications) from single nozzles of standard piezo print-heads are compared in Figures 5 and 6 with response $R(f)$ of equation (2).

The test data results shown in Figure 5, for a single printing nozzle of a standard XJ1001 print-head, were normalized by the average speed value measured between 5 kHz and 6 kHz (not shown above). The solid curve superposed on the Figure 5 data is based on aligning the $m = 5, 6, 7$ and 8 sub-harmonic peaks for equation (2), suggesting that $f_H \approx 188$ kHz; the magnitude of the fitted variations is based on a Q-factor of 7, but required an extra cubic background response to reasonably account for the test data. Reproducibility of these speed measurements was estimated, based on measurements at lower frequencies not shown above, as $\pm 3\%$.

Unsurprisingly, a similar curve closely represents measured data from another XJ1001 print-head as shown in Figure 6 for $Q=6.5$.

The XJ126 device has a much lower operating range (< 8 kHz) that lies within the expected ‘flat background’ range ($B \sim 25-30$ kHz), and so residual oscillations are far less evident in the test data.

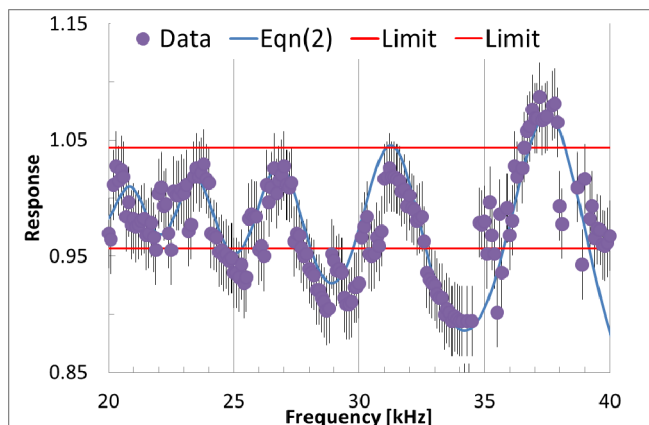


Figure 5. Measurements on drop speed as a function of jetting frequency. The blue curve was computed using Equation 2 (on a cubic background variation), while the data were normalized for comparison purposes to the average speed between 5 kHz and 6 kHz. Agreement with model equation (2) is reasonable.

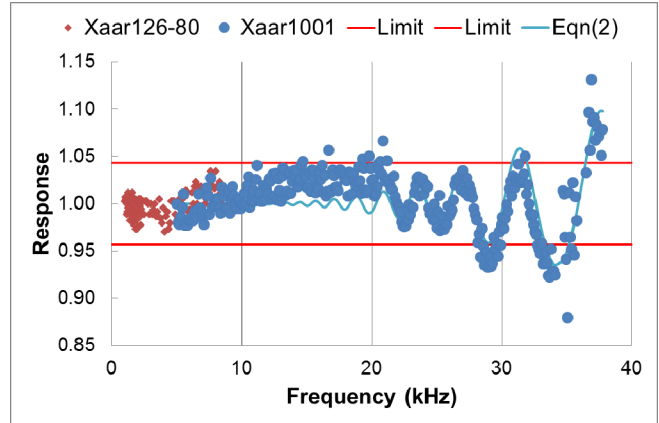


Figure 6. Test data taken for different Xaar series print-heads, showing the normalized drop speed vs. printing frequency, with the typical speed limits and blue curve generated from equation (2) for comparison with the XJ1001 series.

Application to other print-head geometries

Rather more technical comparisons with response measurements on a similar print-head having substantially different [channel and nozzle] geometry are shown in Figure 7. Unlike the previous response speed data shown in Figures 5 and 6, the frequency scale shown in Figure 7 has been suppressed by using $f_H=1$ units, and the two series of data points shown are combinations of response drop speed and response drop volume.

The response function of equation (2) provides predictions for the drop speed and drop volume that are proportional to $R(f)$. So by normalizing drop speeds and volumes measured at low frequency it is straightforward to apply known physical relationships between drop speed, drop volume, drop momentum and drop kinetic energy to deduce momentum and kinetic energy from data and the model:

$$P = \text{Momentum} = \text{mass} \times \text{speed} = R^2 = R^2 \quad (4)$$

$$KE = \text{Kinetic energy} = \text{mass} \times (\text{speed})^2 = R^3 = R^3 \quad (5)$$

Figure 7 shows (with both axes normalized) an example of the application of this simple, output focused, theory to some frequency sweep data obtained for a piezo DoD print-head using a JetXpert system. For this device, the residual response after simple drive pulses revealed the $m = 3, 4, 5$ and 6 sub-harmonics in the derived P and KE (and response) frequency sweeps while the amplitude of the variations imply $Q \sim 5.5$ and hence $B \sim f_H/5.5$. The general agreement between this data and the fitted curves establishes a useful standard benchmark for development devices.

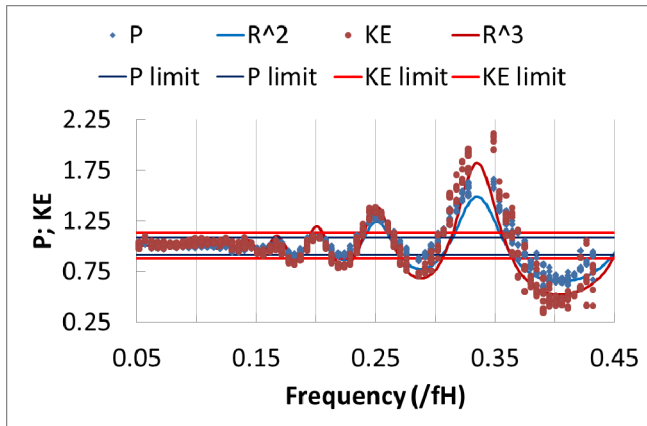


Figure 7. Drop momentum and kinetic energy deduced from measured data for a different DoD print-head geometry compared with model predictions using the equations (4) and (5), as described in the text. Both scales are normalized and show the typical limits on speed applied to the R^2 and R^3 models, respectively.

Comments

Jetting performance depends on the applied drive waveform. Extensions to the multi-pulse train theory for more complex piezo drive waveforms will be reported elsewhere; however the purpose of this simple approach was to capture measurable jetting behavior of piezo DoD inkjet devices without regard to the highly designed pulse waveforms and specific print-head ‘architecture’. Equation (2) has proved particularly useful when incorporated into MatLab fitting of experimental datasets [10]. Dijkstra and Pierik [3] give detailed derivations of the pulse and ramped waveform responses for physical models of fluid motion within simple piezo DoD print head designs. Their math reveals that a ζ -dependent phase angle and absolute amplitude appear in the expression for time-dependent decay following a single pulse. Both these features (phase angle and amplitude) in [3] are absent from the simpler equation (1) due to the normalization of response; however using [3] will produce results equivalent to equation (2). Neither explicit forms of equations (2) and (3), nor the ‘Nth drop’ variations, appear to be discussed elsewhere for inkjet print-heads. The math in Dijkstra and Pierik [3] shows that the results from the derivation of print-head response will depend on the initial state of the meniscus, usually assumed to be correctly positioned within the nozzle and stationary. Relaxing these conditions for every drive pulse beyond the first would be far beyond the simple model, and in some sense does not appear necessary from the data shown in Figures 5-7. However, a better model would take into account more than one resonance mode, as discussed in Khalate et al [11].

Conclusions

Application to inkjet printing provides the following exact results: new predictions of “first drop” effects irrespective of the typical first drop behavior attributed to nozzle blocking or solvent evaporation; the exact general form of the steady state frequency spectrum; residual wave amplitudes in the time domain; the number of jetting pulses required to approach the steady state frequency response curve for a given damping of the resonator; and predictions for certain drive waveforms. No sophisticated

software is required to generate the response curves, facilitating automated fitting to jetting results for development print-heads.

Appendix

When a piezo DoD print-head channel responds to an isolated ‘first’ drive pulse thereby printing a ‘first drop’ it does so from quiescent conditions, assuming there is no interaction or ‘cross-talk’ between that channel and others within the print-head. This pulse produces a print head response that subsequently decays in time, but if a second drive pulse then arrives before the decay was complete, there will be a residual response to add linearly to the second pulse. This scenario can continue indefinitely, but the usual condition is for a period of printing N pulses at a fixed frequency, and for large N corresponds to continuous ‘steady state’ printing. Derivations of the multi-pulse train response can be made by linearly summing N successive pulse responses together, by taking into account the decay and the relative phase of each pulse. The math is analytic because the finite N -pulse sum can be expressed as

$$1+x+\dots+x^n+\dots+x^{(N-1)} = (1-x^N)(1+x+\dots+x^{n-1}) = (1-x^N)/(1-x) \quad (6)$$

where $|x| < 1$.

Equation (6) hides the physical identification of the N th pulse, as corresponding to response amplitude 1 and the very first pulse now having the response $x^{(N-1)}$: the finite series terms appear in reverse time-order. This reversal implies, as it should do, that all ‘first drop’ effects do get lost from the ‘steady state’ printing response.

My math derivation expressed the n th term $\cos(na)\exp(-nb)$ in the series as the complex variable $\exp(\pm jna - nb) = x^n$, where $j = \sqrt{-1}$. Then $(1-x^*) = 1 - \exp(na/(\pm j) - nb)$, the complex conjugate of the summed denominator in equation (6), is used to obtain the solution in terms of the exponentials and the $\cos(a)$ and $\cos(Na)$ factors in equations (2) and (3). More directly, equations (2) and (3) can be found by using the Z-transform [12] of $\cos(na)\exp(-nb)$ for $n \geq 0$.

Acknowledgements

This work was performed under a UK EPSRC Impact Acceleration Knowledge Transfer Fellowship (grant no. EP/K503757/1). Xaar and other consortium members within the I4T (innovation in industrial inkjet technology) project (grant no. EP/H018913/1) gave permission to publish the results and also provided further support. Mario Massucci and Marko Dorrestijn (Xaar Cambridge), and Eva Singler and Ingo Reinhold (Xaar Sweden), all shared their piezo DoD print-head data for this paper.

References

- [1] D. Bogy and F. Talke, “Experimental and theoretical study of wave propagation phenomena in drop-on-demand ink jet devices,” *IBM J. Res. Dev.*, 28, 314–321 (1984).
- [2] J.F. Dijkstra, “Hydrodynamics of small tubular pumps,” *J. Fluid Mech.*, 139, 173–191 (1984).
- [3] J.F. Dijkstra and A. Pierik, *Inkjet Printing Technology for Digital Fabrication* (Hutchings and Martin (Eds), Wiley, 2013) Ch. 3.

- [4] H. Wijshoff, "The dynamics of the piezo inkjet printhead operation", *Physics Reports* 491, 77-177 (2010).
- [5] A. Khalate, X. Bombois, R. Babuška, H. Wijshoff, and R. Waarsing, "Performance improvement of a drop-on-demand inkjet printhead using an optimization-based feedforward control method," *Control Engineering Practice*, 19, 771–781 (2011).
- [6] A. Khalate, X. Bombois, G. Scorletti, R. Babuška, S. Koekebakker, and W. de Zeeuw, "A Waveform Design Method for a Piezo Inkjet Printhead based on Robust Feedforward Control", *IEE, J. Microelectromechanical Systems*, 99, 1-10 (2012).
- [7] N. Morita, A. Khalate, A. van der Buul, and H. Wijshoff, Inkjet Print-heads, in *Fundamentals of Inkjet Printing: The Science of Inkjet and Droplets*, S.D. Hoath (Ed.), Wiley-VCH (2016) Ch. 3
- [8] N. Reis, C. Ainsley, and B. Derby, Inkjet delivery of particle suspensions by piezoelectric droplet ejectors, *J. Appl. Phys.* 97, 094903/1-094903/6 (2005).
- [9] S.D. Hoath, W.-K. Hsiao, S. Jung, G. Martin, I.M. Hutchings, N.F. Morrison, and O.G. Harlen, Drop Speeds from Drop-on-Demand Ink-Jet Print Heads, *J. Imaging Sci. Technol.*, 57, 10503-1-10503-11 (2013).
- [10] T. Cruz-Urbe and M. Dorrestijn (private communications).
- [11] A. Khalate, X. Bombois, G. Scorletti, R. Babuška, S. Koekebakker, and W. de Zeeuw, "A Waveform Design Method for a Piezo Inkjet Printhead based on Robust Feedforward Control", *J. Microelectromechanical Systems* 21, 1365-1374 (2012).
- [12] J.R. Ragazzini and L.A. Zadeh, The analysis of sampled-data systems, *Trans. Am. Inst. Elec. Eng.* 71 (II): 225–234 (1952).

Author Biography

Stephen Hoath took his BA in physics (1972), DPhil in nuclear physics (1977) in Oxford and a Cambridge PhD in (2015). After Lecturing in Physics at the University of Birmingham, Edwards High Vacuum and Cambridge SMEs, he then joined University of Cambridge (2005). Steve, a Chartered Scientist, Physicist and Engineer, Fellow of IOP and Wolfson College, Cambridge, EPSRC Knowledge Transfer Fellow and IEC TC119 member, works in the Department of Engineering Inkjet Research Centre.